文章编号:1000-0550(2018)02-0319-14 DOI: 10.14027/j.issn.1000-0550.2018.037

赫南特冰期古海洋环境转变及其成因机制研究现状

杨向荣,严德天,张利伟,张宝,徐翰文,刘文慧,郧嘉琳
中国地质大学(武汉)构造与油气资源教育部重点实验室,武汉 430070

摘 要 奥陶纪—志留纪转折期是地质历史时期一个重要的时间节点,形成了广为人知的赫南特冰期。该冰期的形成不仅诱发了显生宙第二大的两幕生物绝灭事件,同样使海水中的地球化学元素循环受到强烈的影响,如海洋碳酸盐与大气 CO_2 的循环受到扰动,全球海平面的降低促使水体逐渐富氧化,进而导致海洋水体 Mo、S、U 等同位素值出现波动,而冈瓦纳大陆被冰雪大面积覆盖则削弱了铝硅酸盐岩的风化作用,并限制了陆壳放射性 ^{187}Os、^{87}Sr 同位素向海水的运移。赫南特冰期的成因一直是学界探讨的热点,被归结于风化作用、火山活动的增强或有机碳的大量埋藏等因素,但对冰期的成因机制与持续时间仍具有较多的争论,其原因很多,比如缺乏独立的生物地层单元同时能够控制浅水碳酸盐岩及深水泥页岩区,缺少转折界限处高精度的地球化学信息与全球等时地层格架下的对比,以及未能排除风化作用、成岩作用和构造热事件对古海洋与古气候重建时的扰动等。

关键词 赫南特冰期;古海洋环境;晚奥陶世;生物灭绝

第一作者简介 杨向荣,男,1992 年出生,硕士研究生,沉积学,E-mail: m15727044911@163.com

中图分类号 P534.4 **文献标志码** A

0 引言

奥陶纪—志留纪转折期是一个重要的地质历史时期(图 1),研究发现这个时期全球板块构造形态、古气候条件、古海洋氧化还原条件、生物群类型等都发生了巨大的改变[1-5],同时期在我国南方沉积了一套黑色页岩,并且该套页岩被作为我国页岩气勘探开采的重要层位[6-8]。因此人们逐渐认识到厘清赫南特冰期不仅对了解地球地质历史时期环境的演化及其与生物进化间的协同关系具有重要理论意义,更对华南页岩气开采具有重要指导意义。尽管学者对赫南特冰期的古海洋环境转变与冰期成因机制做了大量工作,但由于涉及内容的广泛性及学科交叉研究的复杂性,对两者之间的相互关系与及触发机制等许多问题仍未得到较好的解决。为此本文力图从地球科学的角度出发,综合国内外的研究成果,阐述奥陶纪—志留纪转折期古海洋元素地球化学循环与古气候转变,并对两者的协同演化关系做出简要的综述评论。

1 赫南特冰期

过去五亿年以来极地地区有三个时期形成了广泛分布的大陆冰川,其中一次就发生在晚奥陶世赫南特时期(约 444 百万年前)。反映该时期气温显著下降及冰盖形成的证据很多,比如 $\delta^{13}C$ 发生了正漂、海平面的下降、凯迪期冰川沉积物与沉积旋回的出现、含有燧石和磷酸盐的碳酸盐岩以及全球海水中的 $\delta^{18}O$ 值比无冰雪覆盖时期要高[1,9-14]。此外,全球的海洋水体循环程度与极地—赤道的温度梯度密切相关,其也可以揭示当时的气候变冷事件,因为温室气候条件不利于温度梯度的形成,进而导致海洋循环的减弱,相反温度下降会促进温度梯度的形成,导致强烈的海洋循环。因此 Pohl 采用 FOAM 重建了奥陶纪时期海洋表层水体以及海洋—大气的循环模式,发现赫南特冰期引发了 11 ℃的气温变化,并导致了强烈的海洋水体循环[15]。通过古 CO_2 含量计算模型[16]以及生物—非生物指标数据[17-19]显示该时期 CO_2 的含量高达 14~22 倍现今的水平,而冰期就发生在这样的高 CO_2 含量时期[20-21]。

2 赫南特冰期的影响

2.1 海洋碳循环

晚寒武世时期全球 C 循环被认为经历了强烈波动[22-23],而这种波动是由不稳定的古海洋氧化还原条件以及间歇性的硫化水体扩张活动引发的[22-25]。到了早—中奥陶世 $\delta^{13}C_{carb}$ 值变得相对稳定[26-27],反映了该时期较稳定的全球 C 循环[28]。到了晚奥陶世

收稿日期: 2017-06-10; **收修改稿日期**: 2017-07-22
基金项目: 国家自然科学基金项目(41690131,41572327,41273001)[**Foundation**: National Natural Science Foundation of China, No. 41690131, 41572327,41273001]

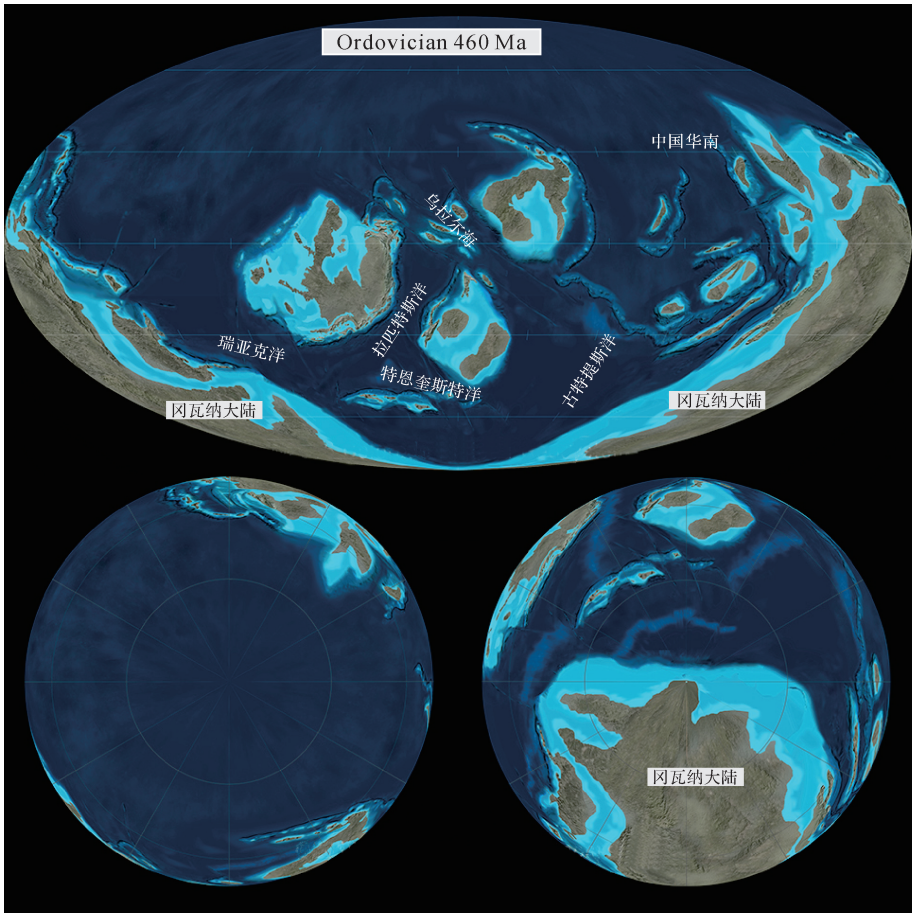

图 1 奥陶纪全球板块复原图(来源于 https://deeptimemaps.com/)

Fig.1 Reconstruction of Gondwana during Ordovician(derived from https://deeptimemaps.com/)

时期全球 C 同位素出现了两次波动即 GICE 和 HICE 事件,上奥陶统古登贝尔阶碳同位素正漂幅度较小(约+2‰~+4‰),而在上奥陶统赫南特阶出现的 $\delta^{13}C_{carb}$ 正漂则更加强烈(约+3‰~+7‰)且持续时间更长(约 1Myr)[23,29-30](图 2)。晚奥陶世赫南特时期全球有机碳同位素 $\delta^{13}C_{org}$(约-1‰)数据显示了较一致的趋势,即晚奥陶世凯迪期 $\delta^{13}C_{org}$ 值保持较稳定的低值,随后在赫南特早期逐渐发生正漂,并在早志留世的鲁丹期 $\delta^{13}C_{org}$ 值重新恢复到凯迪期水平,但是 $\delta^{13}C_{org}$ 漂移事件存在一定的空间差异性,即其开始漂移的位置可以在凯迪阶—赫南特阶界限之下(在 *Dicellograptus mirus* 生物带)[31],也可以在界限处[32]或者在界限之上(中 *M. extraordinarius-N. ojsuensis* 生物带)[33]。HICE 事件的发生被很多研究认为是由于大量有机碳的埋藏[27,34],另一种假设则认为 HICE 事件与暴露地表的碳酸盐岩风化作用有重要内在联系[1,35],但结合钙同位素等信息指示风化作用并不足以引发全球尺度的碳同位素波动[30,36]。两种模式的不同之处在于对赫南特阶冰期空气中 CO_2 分压变化时间节点的确定。在生产力假设中大气 CO_2 分压的下降及冰期的到来是由于海洋生产力的增强,导致富含 ^{12}C 同位素有机碳的大量埋藏并离开了海洋—大气系统,那么海相碳酸盐岩中 C 同位素开始升高处反映了海平面的变化、海洋表面温度的降低、冰川的扩张[2,37-38]。相反,碳酸盐岩风化假设认为空气中 CO_2 分压的下降发生在海相碳酸盐岩中 C 同位素升高之前,这可能是由于强烈的硅酸盐风化或者构造作用引发的火成岩风化对 CO_2 消耗量的增强[39]。最近对美国犹他州和内华达州的五个剖面进行的高精度 $\delta^{13}C_{carb}$ 研究发现,HICE 时期 $\delta^{13}C_{carb}$ 最大值展现了明显的平面梯度,即从盆地中心(+7.5‰)向内陆架地区逐渐减少(+2.5‰)。这种梯度性可能是由于该时期海平面较低,海盆周围隆起地区被剥蚀得更严重,引发了区域性的不整合特征[35]。当然由于不同地质年代以及不同地质相带生活的生物存在一定差异性,因此缺乏较独立的生物地层单元同时能够控制浅水

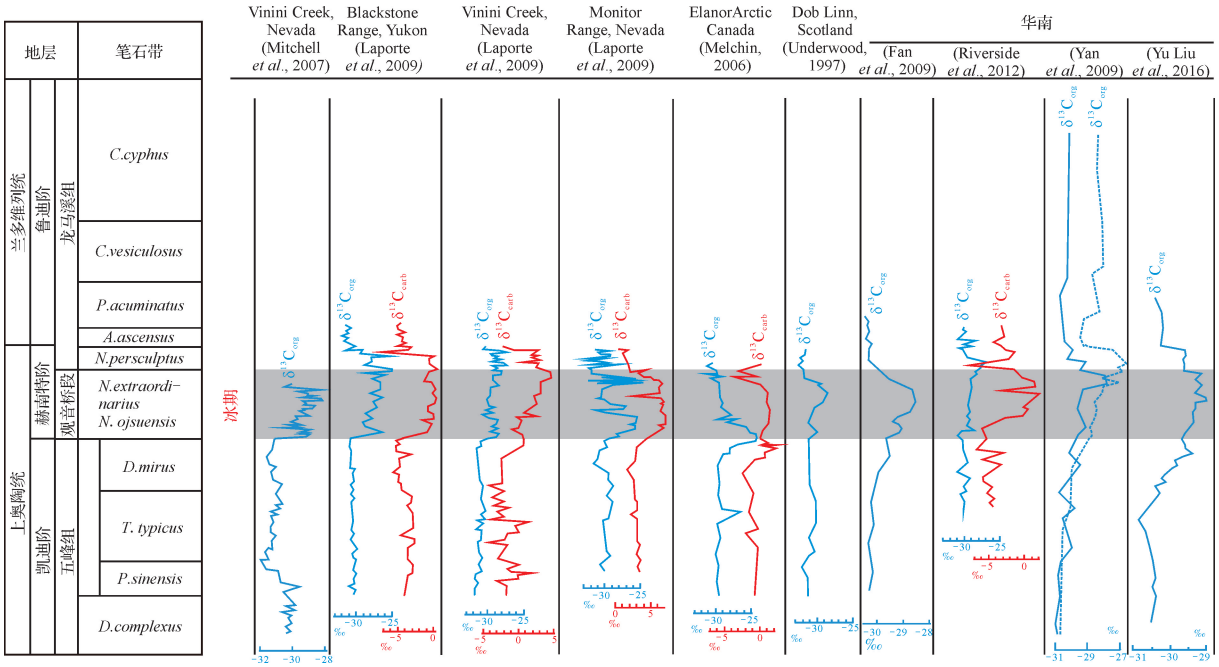

图 2　奥陶纪—志留纪转折期全球碳同位素记录

Fig.2　The variation of carbon isotope during O-S transition

碳酸盐岩及深水泥页岩区,导致有机碳同位素 $\delta^{13}C_{org}$ 与无机碳同位素 $\delta^{13}C_{carb}$ 间存在不一致性,引发学者思考对 HICE 的使用与解释的正确合理性[40]。

2.2　海洋水体硫循环

地球系统中 S 元素的地球化学循环可以解释海相沉积物中硫同位素 $\delta^{34}S$ 波动[41-46],沉积物在硫化或铁化还原水体中通常会发生微生物硫酸盐还原作用(MSR)[47-49],其可以引发海水硫酸盐中 70% 的 ^{34}S 发生分馏[50-52],MSR 作用也被广泛用于解释奥陶纪—志留纪转折期 S 同位素波动特征。同 $\delta^{13}C_{org}$ 变化趋势一样,$\delta^{34}S_{pyrite}$ 在凯迪期阶保持稳定,而在赫南特期发生显著的正漂事件,随后在早志留世鲁丹期重新恢复到冰期之前的水平[3,31,33-34](图 3)。S 同位素与 C 同位素的耦合作用对解释该时期古海洋—古气候变化具有重要意义,Young *et al.*[53] 从阿巴拉契亚盆地记录的中—晚奥陶世 C-S 同位素信息中发现了两次重要波动,即 $\delta^{34}S_{CAS}$ 出现显著(12‰)负偏的同时 $\delta^{34}S_{pyrite}$(+10‰)和 $\delta^{13}C_{carb}$(+2‰)发生了正漂,这种演化关系反映了赫南特时期全球黄铁矿埋藏速率以及海水硫酸盐与沉积黄铁矿间的 S 同位素分异程度降低。引发这些变化的原因很多,一是海洋系统逐渐富氧化,削弱了微生物硫酸盐还原作用(MSR),进而降低了黄铁矿的沉淀量[31,34,54]。此外富黄铁矿沉积物风化作用的增强也是一个可能的因素,但目前还缺少相关的沉积学与地球化学证据能够支持这一假设。

2.3　海洋水体 Os、Sr 循环

海水的 Os 同位素组成反映了两种来源 Os 的相对强弱,一是地壳碎屑物质中高放射性 Os($^{187}Os/^{188}Os_{风尘}=1.05$,$^{187}Os/^{188}Os_{大陆地壳或河流}=1.05$),另一个是来源于大洋地幔圈或地核的低放射性 Os($^{187}Os/^{188}Os_{地幔或地核}=0.13$)[55-58]。Os 元素在海洋中一般存在约 10~40 个千年,相较海洋混合的时间更长,因此使用 Re-Os 体系以及初始 Os 同位素(Os_i)组成可以分析古海洋 Os 循环[58-62],进而反映海洋沉积物来源变化[63-64]。有学者对苏格兰 Dob′s Linn 剖面(GSSP)做了 Os 同位素测定,并用来分析赫南特期古气候变化[65](图 3),发现 *Complanatushe* 和 *anceps* 生物带早期 Os_i 值从 0.28 增高到 1.08,这种具放射性来源的 Os_i(1.08)较整个显生宙甚至是现今海洋来说都是偏高的(~1.06)[63,66-68]。初始 Os 同位素(Os_i)的变化趋势反映了晚奥陶世凯迪期风化作用具有增强的趋势,这很可能会促使大气 CO_2 分压降低,进而引发冰期的形成。而后在赫南特阶底部的 *Extraordinarius* 带开始降低为低放射性来源,这被解释为赫南特阶大陆冰盖的形成降低了化学风化作用的强度[65-66]。

古海洋中 Sr 同位素组成受陆源风化物质与地幔热液流体的影响[69-70],至今很多关于古生代 $^{87}Sr/^{86}Sr$

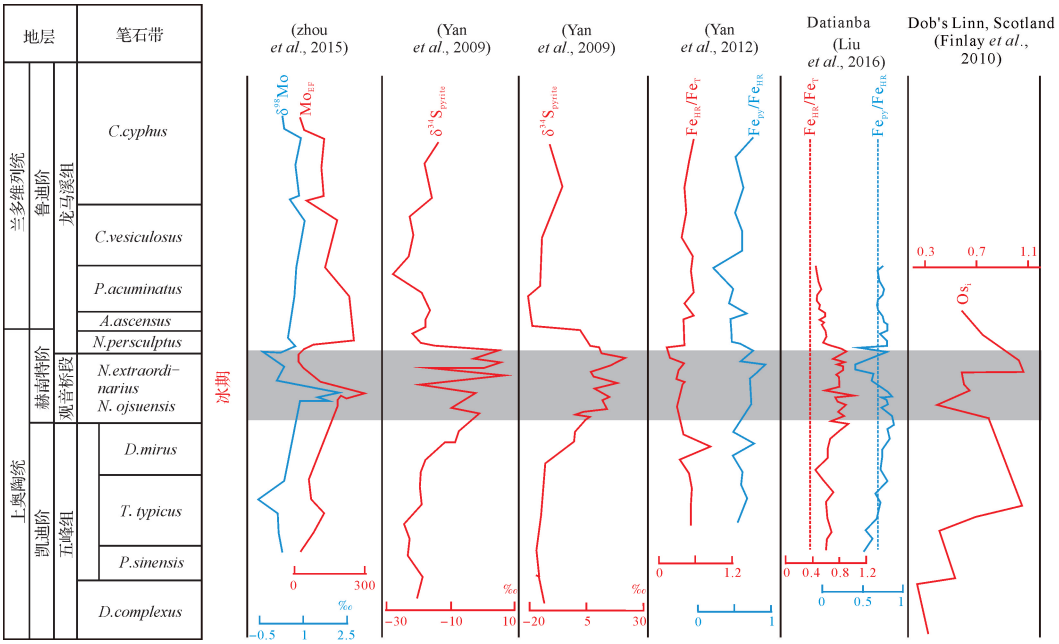

图 3 奥陶纪—志留纪转折期地球化学元素记录

Fig.3 The variation of geochemical proxies during O-S transition

比值研究被用来分析古海洋环境、古构造演化以及古陆风化作用[70-74]。其中上奥陶统沉积物中的$^{87}Sr/^{86}Sr$同位素曲线显示出非常大的波动范围[75](图 4),早—中奥陶世海水$^{87}Sr/^{86}Sr$值开始下降(0.709 0~0.708 8),在晚奥陶世早期骤降为 0.707 8,这也被认为是显生宙以来最大的一次波动[39],随后在晚奥陶世—早志留世时期开始逐渐上升[69,75-76]。如同对新生代$^{87}Sr/^{86}Sr$值波动的解释一样[77-78],大多数人认为奥陶纪晚期$^{87}Sr/^{86}Sr$值的剧烈上升是由于海平面降低、构造造山运动加强,进而引发的大陆风化作用增强[75,78-80]。

2.4 海洋水体氧化还原环境

Mo 元素的含量可以被用来判定全球古海洋氧化还原条件[81-85],而如今使用 Mo 同位素进一步探讨古海洋水体氧化还原条件的演化[86-89]。赫南特冰期 Mo 同位素出现了明显的波动(图 3),从中国南方的王家湾剖面来看,冰期前后具有较高的$\delta^{98}Mo$值,反映了缺氧的海洋环境,而在赫南特时期的一次突降指示了一次水体氧化事件[87,89,90-92]。U 同位素同样可以被用来评估古海洋水体的氧化还原特性[93-97],晚奥陶世晚期与早志留世早期海水中的$\delta^{238}U$被认为大约在-0.60‰到-0.85‰之间,而该时期河流中的$\delta^{238}U$则与现今一致约为-0.3‰[98-100]。通过计算可以发现,缺氧水体中的 U 通量与其他来源的 U 通量分别

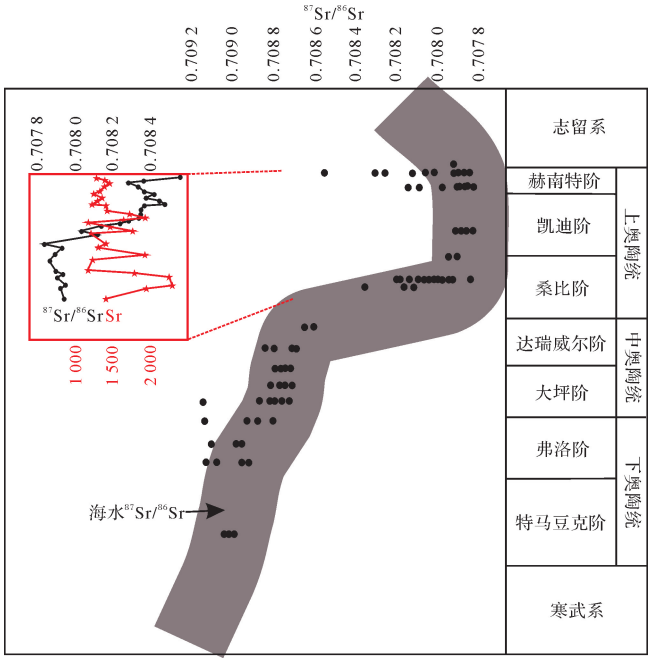

图 4 奥陶纪—志留纪转折期全球 Sr 同位素记录[75-76]

Fig.4 The variation of strontium isotope during O-S transition[75-76]

占据该时期 U 含量的 46%~63%和 37%~54%,并且缺氧水体中的 U 通量是现今海洋中的 4~9 倍,反映冰期前后古海水的严重缺氧[92]。Fe 组分分析是重建海洋水体环境的一种重要手段[101-103],通常认为在

晚奥陶世晚期和早志留早期全球海水的 $Fe_{HR}/Fe_T>0.38$且 $Fe_{py}/Fe_{HR}<0.8$,指示了缺氧铁化的水体环境,而赫南特期的 $Fe_{HR}/Fe_T<0.38$反映了氧化的海洋环境[104](图 3),不过同开阔海的强水体循环不同,在局限海下水体更易形成缺氧的硫化水体[105]。但与先前普遍认为的冰期海水逐渐富氧化不同,有研究发现 Fe 组分特征在整个晚奥陶世包括赫南特时期都指示了一种严重缺氧的环境[106]。

2.5　海洋生物灭绝

赫南特阶被认定为奥陶纪最末期不到 2 Myr 的一段地层[107-108],研究认为 *N. extraordinarius-N. ojsuensis* 带为该阶的下部笔石带[109-110],其底界与 *N. extraordinarius* 和 *N. ojsuensis* 的首现一致。而其后的研究表明这两种笔石的首现并不完全相同,在王家湾北剖面(GSSP)*N. ojsuensis* 的首现位于 *N. extraordinarius* 首现层位之下 4 cm 处,这种先后顺序均可和美国内华达[111]、西伯利亚科累马[112-113]以及哈萨克斯坦南部[114-115]等剖面对比,故而该笔石带改名为 *N. extraordinarius* 带,并作为赫南特阶的底界。赫南特阶的顶界与志留系底界重合,因此赫南特阶就包括下部的 *N. extraordinarius* 带和上部的 *N. persculptus* 带。

该时期生物灭绝事件消除了海洋无脊椎生物中 49%~61%的属以及约 86%的种[116-118],使其成为显生宙以来仅次于 P-T 的第二大生物灭绝事件,在这次灭绝事件中受到强烈波及的生物包括三叶虫、腕足类、笔石、牙形虫、无脊椎珊瑚、几丁虫。并且本次事件可划分为两个阶段,第一幕灭绝发生在赫南特冰期的起始阶段,对应于 445 Ma 前的 *N. extraordinarius-N. ojsuensis* 生物带,并在全球具有有广泛分布[119-122],第一幕导致了 *N. extraordinarius* 带底部的全球范围内的笔石消亡,仅在扬子区是个例外,因此 Mitchell *et al.*[123]认为当时扬子区是笔石的避难所。尽管扬子地区剖面表明此带的灭绝率也很高,但是不少笔石动物群的分子仍然穿越了大灭绝的主幕而延入赫南特阶[124],并且这一灭绝事件发生的时间是穿时的,在浅水区发生得早而深水区则晚[117,124-126]。第二幕则发生在约 444 Ma 前 *N. persculptus* 生物带[4,119-121]。赫南特时期海洋水体以赫南特贝动物群的凉水腕足类为代表,它以命名属赫南特贝 *Hirnantia* 为代表、伴以一些其他独特分子和广布型分子[119],赫南特贝动物群在扬子区从近岸至远岸的一系列产地,首现层位逐渐升高,动物群延续时限越来越短,而多样性却越来越高。纵向考察表明,近岸产地的赫南特贝动物群多样性由高向低演变,而远岸较深水产地的多样性演变则由低变高。随地点和层位而发生的环境因子变化(如水深、底质等),赫南特贝动物群对应于不同的群落、亚群落或群集[127]。赫南特阶时期,海底缺氧范围逐渐收缩,进而削弱了反硝化作用,因此提供了足够的生物氮给喜寒的真核生物,烃类生物标志化合物中的原核生物比例在该时期逐渐降低[128]以及微型浮游生物(疑源类)的增长[129]证明了这个观点,然而这样的环境转变非常不利于喜好高营养成分、低氧含量的笔石生存,导致了它的大面积绝灭[129-131]。即使有学者提出了海底硫化缺氧的环境可能是导致生物灭绝的原因[131],但是人们更愿意相信气候的转变是触发这两幕绝灭事件的诱因。值得注意的是气温的变冷是冰期的直接效果,而海底硫化缺氧环境位置的下移则与冰期海平面的下降有关,因此无论哪种机制都与赫南特冰期的出现息息相关。

3　赫南特冰期的成因机制

3.1　风化作用

地质历史时期大气 CO_2 浓度的缓慢下降可以解释为构造造山运动形成隆起,进而大大增强了硅酸盐岩、玄武岩的风化作用[1],依据海水中 $^{87}Sr/^{86}Sr$ 的比值[39,75]以及 CIA 指数[132],表明其风化速率在早—中奥陶世时期是较强的,但在晚奥陶世开始出现显著的降低。值得注意的是,在冰期开始之前的凯迪期 Os_i 值明显增高[65],这一趋势表明该时期风化作用的增强,并且可以被解释为构造运动的加强引发的大陆硅酸盐风化作用增强。研究发现由于硅酸盐岩风化强度的阶段变化,导致大气中的 CO_2 分压在距今 400~360 Ma 以前的泥盆纪出现了明显的下降,最后导致全球气温下降以及极地的冰期形成[16],因此一些学者就认为晚奥陶世时期岩石的风化作用逐渐增强是触发赫南特冰期形成的重要机制[65,133]。温暖潮湿的温室气候条件可以促使硅酸盐岩化学作用的加剧,另外当大陆板块运动经过赤道地带时,充足的降水量也可以增强风化作用[27]。而近年来发现植物可能是风化作用增强的重要诱因,植物再生长过程中需要吸收矿物质—包括磷酸盐、钾元素、钙元素、镁元素和铁元素,而陆生植物的出现可以加强岩石中重要的营养物质释放,尤其是陆生维管植物的出现大大增强了对含有营养物质的硅酸盐矿物的风化作用[134],比如对钙元素的风化因子就达到 2~10。Timothy *et al.*[135]分别观察了苔藓植物(即无维管植物)与非生物因素控

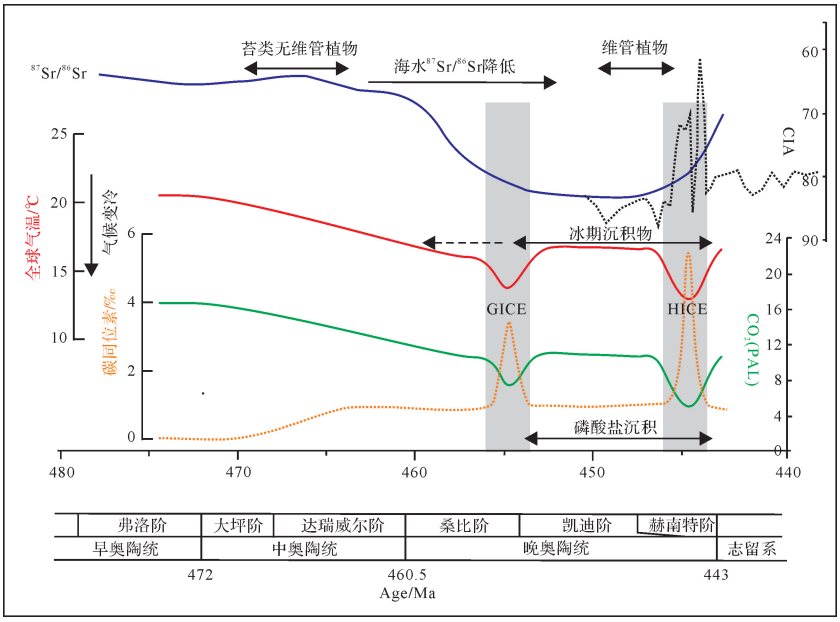

图 5 奥陶纪—志留纪转折期风化作用强度(据 Yan *et al.*[132]; Timothy *et al.*[135]改)

其中红实线、绿实线、橙虚线分别代表依据早期植物的磷酸盐风化作用预测的全球温度、大气 CO_2 分压、碳同位素变化趋势

Fig.5 The intensity of weathering during O-S transition(based on Yan *et al.*[132]; Timothy *et al.*[135])

Model results, predicted Ordovician variations in red solid line, global temperature, green solid line, atmospheric CO_2, and orange dotted line, $\delta^{13}C$ of marine carbonates, for: baseline model with Ordovician adding transient enhancement of phosphorus weathering by early plants

制下的花岗岩和安山岩的风化强度,证实了无维管植物的确可以增强硅酸盐岩的风化作用(图 5),并且利用 COPSE 模型[17]对 480 Ma 以来的 CO_2 水平以及全球气温变化进行了模拟,发现在陆生维管植物与无维管植物的影响下,在约 458 Ma 和 444 Ma 以前出现了两个极低值,分别对应了 GICE 以及 HICE 事件。

3.2 火山作用

研究表明通过火山活动或者变质作用导致的大量的 C 输送到海洋—空气系统中是导致温室气候的一个重要触发机制,而风化作用的加强在很多时代也被认定为剧烈的火山活动所引发,即火山喷发出的大量 CO_2 气体以及易风化的玄武岩都能促进大陆风化作用[136-138]。相较于火山系统,沿着大陆边缘的岩浆弧俯冲带由于将地壳中储存的碳酸盐矿物分解,因而被认为释放了更多的 CO_2 气体到空气中,尽管对于当时这种方式释放的 CO_2 量计算还存在困难,但现今的大陆火山弧释放的 CO_2 量大约为 150 tg C/年,而大洋中脊大约释放 12~60 tg C/年,大洋板内火山释放 1~30 tg C/年[139-141],因此大陆火山弧可能在控制地球地质历史时期的气候转变过程中扮演了重要角色。罗迪尼亚超大陆在约 900 万年以前开始形成,在约 750 万年以前经历了延展隆升期,最终在约 600 万年前开始崩解[142-144]。罗迪尼亚超大陆的存在就反映了大陆弧火山的减少,而随后的崩解就带来了大陆弧火山的增加,大气中 CO_2 含量在寒武纪达到顶峰,而后冈瓦纳大陆在中奥陶世开始形成,大陆弧火山的量再次降低,导致大气 CO_2 含量出现降低[145],并且 McKenzie *et al.*[142]发现年轻碎屑锆石含量的波动与冰期旋回具有一致性。与之前的 CO_2 触发机制不同,Buggisch *et al.*[146]认为火山活动释放的 SO_2 对晚奥陶世赫南特冰期的形成具有重要作用,由于 SO_2 在对流层极易被氧化固定,而在平流层形成的气溶胶则会阻挡太阳热能,引发地球表面的温度急剧下降,这样来看晚奥陶世凯迪期火山活动的减弱或许是触发冰室气候的关键条件。

3.3 有机碳埋藏

赫南特冰期与有机碳埋藏速率的加强存在一定的联系,即冰期前海洋生物死亡促进了大量有机碳埋藏[31,147-148],进而导致大气 CO_2 分压下降[20,149]。Rosenau *et al.*[150]在古登贝尔阶 GICE 时期发现了较高的 $\delta^{18}O$ 值,认为该时期 $\delta^{18}O$ 值增加了 1.5‰,随后降低为 19.0‰,并在其附近波动,这些结果表明在 GICE 时期内存在短期的冷却事件,因此凯迪阶前(赫南特阶前)出现的古登贝尔 C 同位素正漂

(GICE)就可能是赫南特冰期的一个前奏[11,27,148],这个时期海平面明显上升,碳酸盐沉积从热带过渡到温带[148,151],磷酸盐和硅质沉积增多[11,151]。桑迪阶与凯迪阶界限附近的 GICE 事件可能代表了全球范围内的有机碳埋藏的加强[12,27,39],而晚凯迪期 $\delta^{13}C_{org}$ 值的大幅度变化又反映了低于晚奥陶世冰盖形成的临界 pCO_2 阈值[21,148-149]。同样的,GICE 期后有机碳持续埋藏,CO_2 分压继续降低,最终引发了时间更长、强度更大的赫南特阶碳同位素波动 HICE 与冰期。在这样的模式中,中奥陶世到晚奥陶世存在一个气候逐渐降低的平台,代表了 CO_2 分压在地质时间尺度上的累积降低,直到其突破所需的临界值后,触发了赫南特期出现短暂的气温陡降[133],这就排除了该时期火山活动引发的气候突变[152]。

3.4　其他地质事件

Herrmann *et al.*[153] 认为晚奥陶世古地理和 CO_2 浓度的协同作用,加上海平面的下降、极地海洋热传送的减少导致冰盖的形成,进而触发了全球气温降低。冰川海洋以及大陆沉积物在时空上的分布指示了冰期始于中奥陶世,同时沉积学和动物形态特征也表明了晚奥陶世温暖水体向寒冷水体的转变[154-157],但是这种转变模式存在一定问题,因为根据古地理重建和古气候指标,当时的北美处于热带到亚热带的纬度范围。而晚奥陶世冈瓦纳大陆的向南移动和海平面的下降可能导致了南大洋的热传导减少,最终引发了冈瓦纳冰期的形成或者加强[153]。同时,诸如早期较弱的太阳光照强度[158]、由宇宙射线引发的云层反射率高低[159]也被用来解释气温骤降。值得注意的是全球的氮循环转变可能是触发冰期的重要机制之一,这是因为固氮作用速率以及相伴生的氧化氮的产量对气候环境显得尤为重要[160],氧化氮(N_2O)是一种强有力的温室气体,其引发温室气候的效力是同等量 CO_2 的 300 倍,并且在大气中的持续时间也超过了 100 年[161-162]。因此当 N_2O 这一产物大量减少时,就有助于全球气温变冷甚至是冰期的到来。即使赫南特冰期的结束被归结于大气 CO_2 含量的上升[1],但是也有可能海相氮循环在这一事件中扮演了重要的角色[161],因为在全世界多个剖面的赫南特冰期结束位置都出现了 $\delta^{15}N$ 的漂移[30,129],这一信号反映了该时期反硝化作用的增强,进而导致更多的 N_2O 被释放到大气中增强了温室效应,导致冰期的结束。

4　不同地质作用耦合关系

地球作为一个整体系统,地质历史时期发生的各种地质过程会相互作用、相互影响、相互制约。晚奥陶世火山活动较为频繁,火山喷发出大量的 CO_2 气体,这一过程能引发强烈的大陆铝硅酸盐化学风化作用[65,128]。那么火山活动之后风化作用的增强就可以解释晚奥陶世时期大量陆壳放射性 ^{187}Os、^{87}Sr 同位素向海水的运移,进而引发该时期 ^{187}Os/^{188}Os 与 ^{87}Sr/^{86}Sr 的升高[65,75-76]。但长时期强烈的风化作用便会大量消耗 CO_2,使得大气 CO_2 分压持续降低,加上火山活动喷发的 SO_2 在平流层形成的气溶胶会阻挡太阳热能[148],可以引发全球气温降低。气温的降低能加剧海洋系统的循环,海洋表层与底层水体的循环会促进营养物质的循环,进而诱发高的生物生产力与有机碳埋藏,这一过程不仅能进一步降低大气 CO_2 分压水平,促进气温的降低,并且有机碳的下沉过程还会大量消耗海水中的氧气,在陆棚处形成缺氧的底层水体[31,104]。赫南特时期生物的绝灭事件众多学者有不同的解释,比如有人认为该时期海洋硫化水体的偏移使得大量海洋生物不适应新的生活环境发生了灭绝[5],而更多的学者则将其归咎于赫南特时期气温的骤降引发了显生宙以来第一次生物灭绝事件。

5　存在问题

对于这一地质转折期古气候条件的研究还存在很多争论:

利用碳同位素[19,163]及显生宙碳循环模型[163-166]等古气候条件恢复都显示晚奥陶世时期整体处于一个高 CO_2 分压条件(>8 PAL),但有趣的是依据前人设计的复杂环境模型表明只有当 CO_2 分压下降到 8 PAL 时才会引发冰期的形成[20-21],这种矛盾性的存在可能受限于计算得到的 CO_2 分压曲线的精度,具体原因还有待考证。

Os,Sr 同位素数据显示晚奥陶世时期放射性 ^{187}Os、^{87}Sr 含量逐渐升高,这被很多人解释为风化作用的升高[65,75-76],但陆源风化指数 CIA 值[132]与 Os_i 指数在凯迪期表现出明显不同的变化趋势,加之上奥陶统五峰组发育多层钾质斑脱岩,反映了大规模的火山喷发活动[167],那么晚奥陶世凯迪晚期海洋水体中放射性 ^{187}Os 含量增高[65]或许指示了火山作用的减弱,而非风化作用的增强,总之目前对该时期大陆风化作用与火山作用的耦合关系,尤其是火山活动对海洋环境的影响还较为缺乏,其机制值得深思。

研究发现早凯迪期的气温骤降(GICE)后有气温的回暖[146],这就为有机碳埋藏的时间尺度与冰期开

始的时间节点提出了新的异议。另外诸如对冰期持续的时间长短存在差异性;志留纪之初的气候是迅速变暖还是持续寒冷也有不同的解释和结论;生物演化、海洋环境与气候转变如何相互影响与制约有待研究。而如此多的争论存在的原因很多,比如缺乏独立的生物地层单元同时能够控制浅水碳酸盐岩及深水泥页岩区,缺少转折界限处高精度的地球化学信息与全球等时地层格架下的对比,以及风化作用、成岩作用和构造热事件对古海洋与古气候重建时的干扰,这也就需要我们今后更多的工作来克服这些局限性。

参考文献(References)

[1] Kump L R, Arthur M A. Interpreting carbon-isotope excursions: carbonates and organic matter[J]. Chemical Geology, 1999, 161(1/2/3): 181-198.

[2] Brenchley P J, Carden G A, Hints L, et al. High-resolution stable isotope stratigraphy of Upper Ordovician sequences: constraints on the timing of bioevents and environmental changes associated with mass extinction and glaciation[J]. GSA Bulletin, 2003, 115(1): 89-104.

[3] Chen X, Rong J Y, Fan J X, et al. The global boundary stratotype section and point (GSSP) for the base of the Hirnantian stage (the uppermost of the Ordovician system)[J]. Episodes, 2006, 29(3): 183-196.

[4] Fan J X, Peng P A, Melchin M J. Carbon isotopes and event stratigraphy near the Ordovician - Silurian boundary, Yichang, South China[J]. Palaeogeography, Palaeoclimatology, Palaeoecology, 2009, 276(1/2/3/4): 160-169.

[5] Hammarlund E U, Dahl T W, Harper D A T, et al. A sulfidic driver for the end-Ordovician mass extinction[J]. Earth and Planetary Science Letters, 2012, 331-332: 128-139.

[6] Yan D, Wang H, Fu Q L, et al. Organic matter accumulation of Late Ordovician sediments in North Guizhou Province, China: sulfur isotope and trace element evidence[J]. Marine and Petroleum Geology, 2015, 59: 348-358.

[7] Yan D, Wang H, Fu Q L, et al. Geochemical characteristics in the Longmaxi Formation (Early Silurian) of South China: Implications for organic matter accumulation[J]. Marine and Petroleum Geology, 2015, 65: 290-301.

[8] Chen C, Mu C L, Zhou K K, et al. The geochemical characteristics and factors controlling the organic matter accumulation of the Late Ordovician-Early Silurian black shale in the Upper Yangtze Basin, South China[J]. Marine and Petroleum Geology, 2016, 76: 159-175.

[9] Hambrey M J. The late Ordovician - Early Silurian glacial period[J]. Palaeogeography, Palaeoclimatology, Palaeoecology, 1985, 51(1/2/3/4): 273-289.

[10] Littler K, Hesselbo S P, Jenkyns H C. A carbon-isotope perturbation at the Pliensbachian-Toarcian boundary: evidence from the Lias Group, NE England[J]. Geological Magazine, 2010, 147(2): 181-192.

[11] Pope M C, Steffen J B. Widespread, prolonged late middle to Late Ordovician upwelling in North America: a proxy record of glaciation?[J]. Geology, 2003, 31(1): 63-66.

[12] Ainsaar L, Meidla T, Martma T. The middle Caradoc facies and faunal turnover in the Late Ordovician Baltoscandian palaeobasin[J]. Palaeogeography, Palaeoclimatology, Palaeoecology, 2004, 210(2/3/4): 119-133.

[13] Saltzman M R. Phosphorus, nitrogen, and the redox evolution of the Paleozoic oceans[J]. Geology, 2005, 33(7): 573-576.

[14] Elrick M, Reardon D, Labor W, et al. Orbital-scale climate change and glacioeustasy during the early Late Ordovician (pre-Hirnantian) determined from $\delta^{18}O$ values in marine apatite[J]. Geology, 2013, 41(7): 775-778.

[15] Pohl A, Nardin E, Vandenbroucke T R A, et al. High dependence of Ordovician ocean surface circulation on atmospheric CO_2 levels[J]. Palaeogeography, Palaeoclimatology, Palaeoecology, 2016, 458: 39-51.

[16] Berner R A. GEOCARBSULF: a combined model for Phanerozoic atmospheric O_2 and CO_2[J]. Geochimica et Cosmochimica Acta, 2006, 70(23): 5653-5664.

[17] Tobin K J, Bergström S M. Implications of Ordovician ($\approx$460 Myr) marine cement for constraining seawater temperature and atmospheric pCO_2[J]. Palaeogeography, Palaeoclimatology, Palaeoecology, 2002, 181(4): 399-417.

[18] Tobin K J, Bergström S M, De La Garza P. A mid-Caradocian (453 Ma) drawdown in atmospheric pCO_2 without ice sheet development?[J]. Palaeogeography, Palaeoclimatology, Palaeoecology, 2005, 226(3/4): 187-204.

[19] Yapp C J, Poths H. Carbon isotopes in continental weathering environments and variations in ancient atmospheric CO_2 pressure[J]. Earth and Planetary Science Letters, 1996, 137(1/2/3/4): 71-82.

[20] Gibbs M T, Barron E J, Kump L R. An atmospheric pCO_2 threshold for glaciation in the Late Ordovician[J]. Geology, 1997, 25(5): 447-450.

[21] Herrmann A D, Patzkowsky M E, Pollard D. Obliquity forcing with 8-12 times preindustrial levels of atmospheric pCO_2 during the Late Ordovician glaciation[J]. Geology, 2003, 31(6): 485-488.

[22] Saltzman M R, Ripperdan R L, Brasier M D, et al. A global carbon isotope excursion (SPICE) during the Late Cambrian: relation to trilobite extinctions, organic-matter burial and sea level[J]. Palaeogeography, Palaeoclimatology, Palaeoecology, 2000, 162(3/4): 211-223.

[23] Bergström S M, Xu Chen, Schmitz B, et al. First documentation of the Ordovician Guttenberg $\delta^{13}C$ excursion (GICE) in Asia: chemostratigraphy of the Pagoda and Yanwashan formations in southeastern China[J]. Geological Magazine, 2009, 146(1): 1-11.

[24] Hurtgen M T, Pruss S B, Knoll A H. Evaluating the relationship between the carbon and sulfur cycles in the later Cambrian ocean:

an example from the Port au Port Group, western Newfoundland, Canada[J]. Earth and Planetary Science Letters, 2009, 281(3/4): 288-297.

[25] Gill B C, Lyons T W, Young S A, et al. Geochemical evidence for widespread euxinia in the Later Cambrian ocean [J]. Nature, 2011, 469(7328): 80-83.

[26] Edwards C T, Saltzman M R. Carbon isotope ($\delta^{13}C_{carb}$) stratigraphy of the Lower - Middle Ordovician (Tremadocian - Darriwilian) in the Great Basin, western United States: implications for global correlation[J]. Palaeogeography, Palaeoclimatology, Palaeoecology, 2014, 399: 1-20.

[27] Saltzman M R, Young S A. Long-lived glaciation in the Late Ordovician? Isotopic and sequence-stratigraphic evidence from western Laurentia[J]. Geology, 2005, 33(2): 109-112.

[28] Pruss S B, Castagno K A, Fike D A, et al. Carbon isotope ($\delta^{13}C_{carb}$) heterogeneity in deep-water Cambro-Ordovician carbonates, western Newfoundland[J]. Palaeogeography, Palaeoclimatology, Palaeoecology, 2016, 458: 52-62.

[29] Ghienne J F. Late Ordovician sedimentary environments, glacial cycles, and post-glacial transgression in the Taoudeni Basin, West Africa[J]. Palaeogeography, Palaeoclimatology, Palaeoecology, 2003, 189(3/4): 117-145.

[30] LaPorte D F, Holmden C, Patterson W P, et al. Local and global perspectives on carbon and nitrogen cycling during the Hirnantian glaciation[J]. Palaeogeography, Palaeoclimatology, Palaeoecology, 2009, 276(1/2/3/4): 182-195.

[31] Yan D T, Chen D Z, Wang Q C, et al. Carbon and sulfur isotopic anomalies across the Ordovician - Silurian boundary on the Yangtze Platform, South China[J]. Palaeogeography, Palaeoclimatology, Palaeoecology, 2009, 274(1/2): 32-39.

[32] Melchin M J, Holmden C. Carbon isotope chemostratigraphy in Arctic Canada: sea-level forcing of carbonate platform weathering and implications for Hirnantian global correlation[J]. Palaeogeography, Palaeoclimatology, Palaeoecology, 2006, 234(2/3/4): 186-200.

[33] Zhang T G, Shen Y A, Zhan R B, et al. Large perturbations of the carbon and sulfur cycle associated with the Late Ordovician mass extinction in South China[J]. Geology, 2009, 37(4): 299-302.

[34] Zhang T G, Trela W, Jiang S Y, et al. Major oceanic redox condition change correlated with the rebound of marine animal diversity during the Late Ordovician[J]. Geology, 2011, 39(7): 675-678.

[35] Jones D S, Fike D A, Finnegan S, et al. Terminal Ordovician carbon isotope stratigraphy and glacioeustatic sea-level change across Anticosti Island (Québec, Canada)[J]. GSA Bulletin, 2011, 123(7/8): 1645-1664.

[36] Holmden C, Panchuk K, Finney S C. Tightly coupled records of Ca and C isotope changes during the Hirnantian glaciation event in an epeiric sea setting[J]. Geochimica et Cosmochimica Acta, 2012, 98: 94-106.

[37] Brenchley P J, Carden G A F, Marshall J D. Environmental changes associated with the "first strike" of the Late Ordovician mass extinction[J]. Modern Geology, 1995, 20: 69-82.

[38] Brenchley P J, Marshall J D, Carden G A F, et al. Bathymetric and isotopic evidence for a short - lived Late Ordovician glaciation in a greenhouse period[J]. Geology, 1994, 22(4): 295-298.

[39] Young S A, Saltzman M R, Foland K A, et al. A major drop in seawater $^{87}Sr/^{86}Sr$ during the Middle Ordovician (Darriwilian): links to volcanism and climate? [J]. Geology, 2009, 37(10): 951-954.

[40] DesrochersA, Farley C, Achab A, et al. A far-field record of the end Ordovician glaciation: the Ellis Bay formation, Anticosti Island, eastern Canada[J]. Palaeogeography, Palaeoclimatology, Palaeoecology, 2010, 296(3/4): 248-263.

[41] Burdett J W, Arthur M A, Richardson M. A Neogene seawater sulfur isotope age curve from calcareous pelagic microfossils[J]. Earth and Planetary Science Letters, 1989, 94(3/4): 189-198.

[42] Strauss H. The isotopic composition of sedimentary sulfur through time[J]. Palaeogeography, Palaeoclimatology, Palaeoecology, 1997, 132(1/2/3/4): 97-118.

[43] Ho T Y, Rogers M A, Drushel H V, et al. Evolution of sulfur compounds in crude oils[J]. AAPG Bulletin, 1974, 58(11): 2338-2348.

[44] Yang C, Hutcheon I, Krouse H R. Fluid inclusion and stable isotopic studies of thermochemical sulphate reduction from Burnt Timber and Crossfield East gas fields in Alberta, Canada[J]. Bulletin of Canadian Petroleum Geology, 2001, 49(1): 149-164.

[45] Yuan S D, Chou I M, Burruss R C. Disproportionation and thermochemical sulfate reduction reactions in S - H_2O - CH_4 and S - D_2O - CH_4 systems from 200 to 340°C at elevated pressures[J]. Geochimica et Cosmochimica Acta, 2013, 118: 263-275.

[46] Xia X Y, Ellis G S, Ma Q S, et al. Compositional and stable carbon isotopic fractionation during non-autocatalytic thermochemical sulfate reduction by gaseous hydrocarbons[J]. Geochimica et Cosmochimica Acta, 2014, 139: 472-486.

[47] Canfield D E, Thamdrup B. The production of ^{34}S-depleted sulfide during bacterial disproportionation of elemental sulfur[J]. Science, 1994, 266(5193): 1973-1975.

[48] Habicht K S, Canfield D E, Rethmeier J. Sulfur isotope fractionation during bacterial reduction and disproportionation of thiosulfate and sulfite[J]. Geochimica et Cosmochimica Acta, 1998, 62(15): 2585-2595.

[49] Strauss H. Geological evolution from isotope proxy signals-sulfur[J]. Chemical Geology, 1999, 161(1/2/3): 89-101.

[50] Wortmann U G, Bernasconi S M, Böttcher M E. Hypersulfidic deep biosphere indicates extreme sulfur isotope fractionation during single-step microbial sulfate reduction[J]. Geology, 2001, 29(7): 647-650.

[51] Canfield D E, Farquhar J, Zerkle A L. High isotope fractionations during sulfate reduction in a low-sulfate euxinic ocean analog[J]. Geology, 2010, 38(5): 415-418.

[52] Sim M S, Bosak T, Ono S. Large sulfur isotope fractionation does not require disproportionation[J]. Science, 2011, 333(6038):

74-77.

[53] Young S A, Gill B C, Edwards C T, et al. Middle-Late Ordovician (Darriwilian-Sandbian) decoupling of global sulfur and carbon cycles: isotopic evidence from eastern and southern Laurentia[J]. Palaeogeography, Palaeoclimatology, Palaeoecology, 2016, 458: 118-132.

[54] Kah L C, Thompson C K, Henderson M A, et al. Behavior of marine sulfur in the Ordovician[J]. Palaeogeography, Palaeoclimatology, Palaeoecology, 2016, 458: 133-153.

[55] Pegram W J, Krishnaswami S, Ravizza G E, et al. The record of sea water $^{187}Os/^{186}Os$ variation through the Cenozoic[J]. Earth and Planetary Science Letters, 1992, 113(4): 569-576.

[56] Esser B K, Turekian K K. The osmium isotopic composition of the continental crust[J]. Geochimica et Cosmochimica Acta, 1993, 57 (13): 3093-3104.

[57] Peucker-Ehrenbrink B, Ravizza G. The marine osmium isotope record[J]. Terra Nova, 2000, 12(5): 205-219.

[58] Cohen A S. The rhenium-osmium isotope system: applications to geochronological and palaeoenvironmental problems[J]. Journal of the Geological Society, 2004, 161(4): 729-734.

[59] Kendall B, Creaser R A, Selby D. ^{187}Re-^{187}Os geochronology of Precambrian organic-rich sedimentary rocks[J]. Geological Society, London, Special Publications, 2009, 326(1): 85-107.

[60] Rooney A D, Macdonald F A, Strauss J V, et al. Re-Os geochronology and coupled Os-Sr isotope constraints on the Sturtian snowball Earth[J]. Proceedings of the National Academy of Sciences of the United States of America, 2014, 111(1): 51-56.

[61] Tripathy G R, Hannah J L, Stein H J, et al. Re-Os age and depositional environment for black shales from the Cambrian-Ordovician boundary, Green Point, western Newfoundland[J]. Geochemistry, Geophysics, Geosystems, 2014, 15(4): 1021-1037.

[62] Xu G P, Hannah J L, Stein H J, et al. Cause of Upper Triassic climate crisis revealed by Re-Os geochemistry of Boreal black shales[J]. Palaeogeography, Palaeoclimatology, Palaeoecology, 2014, 395: 222-232.

[63] Turgeon S C, Creaser R A. Cretaceous oceanic anoxic event 2 triggered by a massive magmatic episode[J]. Nature, 2008, 454 (7202): 323-326.

[64] Tejada M L G, Suzuki K, Kuroda J, et al. Ontong Java Plateau eruption as a trigger for the early Aptian oceanic anoxic event[J]. Geology, 2009, 37(9): 855-858.

[65] FinlayA J, Selby D, Gröcke D R. Tracking the Hirnantian glaciation using Os isotopes[J]. Earth and Planetary Science Letters, 2010, 293(3/4): 339-348.

[66] Peucker-Ehrenbrink B, Hannigan R E. Effects of black shale weathering on the mobility of rhenium and platinum group elements [J]. Geology, 2000, 28(5): 475-478.

[67] Oxburgh R, Pierson-Wickmann A C, Reisberg L, et al. Climate-correlated variations in seawater $^{187}Os/^{188}Os$ over the past 200,000 yr: Evidence from the Cariaco Basin, Venezuela[J]. Earth and Planetary Science Letters, 2007, 263(3/4): 246-258.

[68] Selby D, Mutterlose J, Condon D J. U-Pb and Re-Os geochronology of the Aptian/Albian and Cenomanian/Turonian stage boundaries: implications for timescale calibration, osmium isotope seawater composition and Re-Os systematics in organic-rich sediments [J]. Chemical Geology, 2009, 265(3/4): 394-409.

[69] Veizer J, Ala D, Azmy K, et al. $^{87}Sr/^{86}Sr$, $\delta^{13}C$ and $\delta^{18}O$ evolution of Phanerozoic seawater[J]. Chemical Geology, 1999, 161 (1/2/3): 59-88.

[70] McArthur J M, Howarth R J, Bailey T R. Strontium isotope stratigraphy: LOWESS version 3: best fit to the marine Sr-isotope curve for 0-509 Ma and accompanying look-up table for deriving numerical age[J]. The Journal of Geology, 2001, 109(2): 155-170.

[71] Veizer J, Compston W. $^{87}Sr/^{86}Sr$ composition of seawater during the Phanerozoic[J]. Geochimica et Cosmochimica Acta, 1974, 38 (9): 1461-1484.

[72] Burke W H, Denison R E, Hetherington E. A, et al. Variation of seawater $^{87}Sr/^{86}Sr$ throughout Phanerozoic time[J]. Geology, 1982, 10(10): 516-519.

[73] Veizer J. Strontium isotopes in seawater through time[J]. Annual Review of Earth and Planetary Sciences, 1989, 17: 141-167.

[74] Dennison R E, Koepnick R B, Burke W H, et al. Construction of the Cambrian and Ordovician seawater $^{87}Sr/^{86}Sr$ curve[J]. Chemical Geology, 1998, 152(3/4): 325-340.

[75] Shields G A, Carden G A F, Veizer J, et al. Sr, C, and O isotope geochemistry of Ordovician brachiopods: a major isotopic event around the Middle - Late Ordovician transition[J]. Geochimica et Cosmochimica Acta, 2003, 67(11): 2005-2025.

[76] Ruppel S C, James E W, Barrick J E, et al. High-resolution $^{87}Sr/^{86}Sr$ chemostratigraphy of the Silurian: implications for event correlation and strontium flux[J]. Geology, 1996, 24(9): 831-834.

[77] Koepnick R B, Burke W H, Denison R E, et al. Construction of the seawater $^{87}Sr^{86}Sr$ curve for the Cenozoic and Cretaceous: supporting data[J]. Chemical Geology: Isotope Geoscience Section, 1985, 58(1/2): 55-81.

[78] Palmer M R, Elderfield H. Sr isotope composition of sea water over the past 75 Myr[J]. Nature, 1985, 314(6011): 526-528.

[79] Qing H R, Barnes C R, Buhl D, et al. The strontium isotopic composition of Ordovician and Silurian brachiopods and conodonts: relationships to geological events and implications for coeval seawater [J]. Geochimica et Cosmochimica Acta, 1998, 62(10): 1721-1733.

[80] Hannigan R, Brookfield M E, Basu A R. A detailed $^{87}SR/^{86}SR$ isotopic curve for the mid-Cincinnatian (Upper Katian - Lower Hirnantian, Upper Ordovician), NE North American Shelf (Ontario, Canada) transition to the Hirnantian glaciation[J]. Chemical Geology, 2010, 277(3/4): 336-344.

[81] Crusius J, Calvert S, Pedersen T, et al. Rhenium and molybdenum enrichments in sediments as indicators of oxic, suboxic and sulfidic conditions of deposition[J]. Earth and Planetary Science Letters, 1996, 145(1/2/3/4): 65-78.

[82] Algeo T J, Maynard J B. Trace-element behavior and redox facies in core shales of Upper Pennsylvanian Kansas-type cyclothems[J]. Chemical Geology, 2004, 206(3/4): 289-318.

[83] Scott C, Lyons T W, Bekker A, et al. Tracing the stepwise oxygenation of the Proterozoic ocean[J]. Nature, 2008, 452(7186): 456-459.

[84] Scott C, Lyons T W. Contrasting molybdenum cycling and isotopic properties in euxinic versus non-euxinic sediments and sedimentary rocks: refining the paleoproxies[J]. Chemical Geology, 2012, 324-325: 19-27.

[85] Reinhard C T, Planavsky N J, Robbins L J, et al. Proterozoic ocean redox and biogeochemical stasis[J]. Proceedings of the National Academy of Sciences of the United States of America, 2013, 110(14): 5357-5362.

[86] Arnold G L, Anbar A D, Barling J, et al. Molybdenum isotope evidence for widespread anoxia in Mid-Proterozoic oceans[J]. Science, 2004, 304(5667): 87-90.

[87] Dahl T W, Canfield D E, Rosing M T, et al. Molybdenum evidence for expansive sulfidic water masses in ~ 750 Ma oceans[J]. Earth and Planetary Science Letters, 2011, 311(3/4): 264-274.

[88] Kendall B, Gordon G W, Poulton S W, et al. Molybdenum isotope constraints on the extent of late Paleoproterozoic ocean euxinia[J]. Earth and Planetary Science Letters, 2011, 307(3/4): 450-460.

[89] Kendall B, Komiya T, Lyons T W, et al. Uranium and molybdenum isotope evidence for an episode of widespread ocean oxygenation during the late Ediacaran Period[J]. Geochimica et Cosmochimica Acta, 2015, 156: 173-193.

[90] Zhou L, Wignall P B, Su J, et al. U/Mo ratios and $\delta^{98/95}$Mo as local and global redox proxies during mass extinction events[J]. Chemical Geology, 2012, 324-325: 99-107.

[91] Zhou L, Algeo T J, Shen J, et al. Changes in marine productivity and redox conditions during the Late Ordovician Hirnantian glaciation[J]. Palaeogeography, Palaeoclimatology, Palaeoecology, 2015, 420: 223-234.

[92] Lu X Z, Kendall B, Stein H J, et al. Marine redox conditions during deposition of Late Ordovician and Early Silurian organic-rich mudrocks in the Siljan ring district, central Sweden[J]. Chemical Geology, 2017, 457: 75-94.

[93] Montoya-Pino C, Weyer S, Anbar A D, et al. Global enhancement of ocean anoxia during Oceanic Anoxic Event 2: a quantitative approach using U isotopes[J]. Geology, 2010, 38(4): 315-318.

[94] Brennecka G A, Herrmann A D, Algeo T J, et al. Rapid expansion of oceanic anoxia immediately before the end-Permian mass extinction[J]. Proceedings of the National Academy of Sciences of the United States of America, 2011, 108(43): 17631-17634.

[95] Partin C A, Bekker A, Planavsky N J, et al. Large-scale fluctuations in Precambrian atmospheric and oceanic oxygen levels from the record of U in shales[J]. Earth and Planetary Science Letters, 2013, 369-370: 284-293.

[96] Andersen M B, Romaniello S, Vance D, et al. A modern framework for the interpretation of $^{238}U/^{235}U$ in studies of ancient ocean redox[J]. Earth and Planetary Science Letters, 2014, 400: 184-194.

[97] Stirling C H, Andersen M B, Warthmann R, et al. Isotope fractionation of ^{238}U and ^{235}U during biologically-mediated uranium reduction[J]. Geochimica et Cosmochimica Acta, 2015, 163: 200-218.

[98] Andersen M B, Elliott T, Freymuth H, et al. The terrestrial uranium isotope cycle[J]. Nature, 2015, 517(7534): 356-359.

[99] Dhuime B, Wuestefeld A, Hawkesworth C J. Emergence of modern continental crust about 3 billion years ago[J]. Nature Geoscience, 2015, 8(7): 552-555.

[100] Tang M, Chen K, Rudnick R L. Archean upper crust transition from mafic to felsic marks the onset of plate tectonics[J]. Science, 2016, 351(6271): 372-375.

[101] Raiswell R, Canfield D E. Sources of iron for pyrite formation in marine sediments[J]. American Journal of Science, 1998, 298(3): 219-245.

[102] Lyons T W, Severmann S. A critical look at iron paleoredox proxies: new insights from modern euxinic marine basins[J]. Geochimica et Cosmochimica Acta, 2006, 70(23): 5698-5722.

[103] Li C, Love G D, Lyons T W, et al. A stratified redox model for the Ediacaran ocean[J]. Science, 2010, 328(5974): 80-83.

[104] Yan D T, Chen D Z, Wang Q C, et al. Predominance of stratified anoxic Yangtze Sea interrupted by short-term oxygenation during the Ordo-Silurian transition[J]. Chemical Geology, 2012, 291: 69-78.

[105] Liu Y, Li C, Algeo T J, et al. Global and regional controls on marine redox changes across the Ordovician-Silurian boundary in South China[J]. Palaeogeography, Palaeoclimatology, Palaeoecology, 2016, 463: 180-191.

[106] AhmA S C, Bjerrum C J, Hammarlund E U, et al. Disentangling the record of diagenesis, local redox conditions, and global seawater chemistry during the latest Ordovician glaciation[J]. Earth and Planetary Science Letters, 2017, 459: 145-156.

[107] Williams S H. The Ordovician-Silurian Boundary graptolite fauna of Dob´s linn, southern Scotland[J]. Palaeontology, 1983, 26: 605-630.

[108] Gradstein F M, Ogg J G, Smith A G, et al. A new geologic time scale, with special reference to Precambrian and Neogene[J]. Episodes, 2004, 27(2): 83-100.

[109] Rong J Y, Chen X, Harper D A T, et al. Proposal of a GSSP candidate section in the Yangtze Platform region, S. China, for a new Hirnantian boundary stratotype[J]. Acta Universitatis Carolinae Geologica, 1999, 43(1/2): 77-80.

[110] Chen X, Rong J Y, Mitchell C E, et al. Late Ordovician to earliest Silurian graptolite and brachiopod biozonation from the Yangtze region, South China, with a global correlation[J]. Geological Magazine, 2000, 137(6): 623-650.

[111] Finney S C, Berry W B N, Cooper J D, et al. Late Ordovician mass extinction: a new perspective from stratigraphic sections in central Nevada[J]. Geology, 1999, 27(3): 215-218.

[112] Koren T N, Oradovskaya M M, Sobolevskaya R F. The Ordovician-Silurian boundary beds of the north-east USSR[M]//Cocks L R M, Rickards R B. A Global Analysis of the Ordovician-Silurian Boundary. Bulletin of British Museum (Natural History), Geology, 1988,43: 133-138.

[113] Koren T N, Oradovskaya M M, Sobolevskaya R F, et al. The Ordovician and Silurian boundary in the Northeast of the USSR[J]. Trudy Mezhvedomstvennogo Stratigraficheskogo Komiteta SSSR, 1983, 11: 1-205. (in Russian)

[114] Koren T N, Sobolevskaya R F, Mikhajlova N F, et al. New evidence on graptolite succession across the Ordovician-Silurian Boundary in the Asian part of the USSR[J]. Acta Palaeontologica Polonica, 1979, 24(1): 125-136.

[115] Apollonov M K, Bandaletov S M, Nikitin J F. The Ordovician-Silurian Boundary in Kazakhstan[M]. Alma-ata: "Nauka" Kazakhstan SSR Publishing House, 1980: 1-232. (in Russian)

[116] Jablonski D. Extinctions: a paleontological perspective[J]. Science, 1991, 253(5021): 754-757.

[117] Sheehan P M. The Late Ordovician mass extinction[J]. Annual Review of Earth and Planetary Sciences, 2001, 29: 331-364.

[118] Harper D A T. The Ordovician brachiopod radiation: roles of alpha, beta, and gamma diversity[M]//Finney S C, Berry W B N. The Ordovician Earth System, Volume 466. Boulder, Colorado: Geological Society of America, 2010: 69-83.

[119] Rong J Y. Distribution of the *Hirnantia* fauna and its meaning [M]//Bruton D L. Aspects of the Ordovician System. Palaeontological Contributions from the University of Oslo 295. Oslo: Universitetsforlaget, 1984: 101-112.

[120] Rong J Y, Chen X, Harper D A T. The latest Ordovician *Hirnantia* fauna (Brachiopoda) in time and space[J]. Lethaia, 2002, 35(3): 231-249.

[121] Harper D A T, Hammarlund E U, Rasmussen C M Ø. End Ordovician extinctions: a coincidence of causes[J]. Gondwana Research, 2014, 25(4): 1294-1307.

[122] Zhan R B, Liu J B, Percival I G, et al. Biodiversification of Late Ordovician *Hirnantia* Fauna on the upper Yangtze platform, South China[J]. Science China: Earth Sciences, 2010, 53(12): 1800-1810.

[123] Mitchell C E, Melchin M J, Sheets H D, et al. Was the Yangtze Platform a refugium for graptolites during the Hirnantian (Late Ordovician) mass extinction? [M]//Albanesi G L, Beresi M S, Peralta S H. Ordovician from the Andes. Tucumán, Argentina: Universidad Nacional de Tucuman, 2003: 523-526.

[124] Chen X, Melchin M J, Sheets H D, et al. Patterns and processes of latest Ordovician graptolite extinction and recovery based on data from South China[J]. Journal of Paleontology, 2005, 79(5): 842-861.

[125] Brenchley P J, Pickerill P K. Animal-sediment relationships in the Ordovician and Silurian of the Welsh Basin[J]. Proceedings of the Geologists' Association, 1993, 104(2): 81-93.

[126] Harper D A T, Rong J Y. Patterns of change in the brachiopod faunas through the Ordovician-Silurian interface[J]. Modern Geology, 1995, 20: 83-100.

[127] 詹仁斌,刘建波,Percival I G,等. 华南上扬子区晚奥陶世赫南特贝动物群的时空演变[J]. 中国科学:地球科学,2010,40(9):1154-1163. [Zhan Renbin, Liu Jianbo, Percival I G, et al. Biodiversification of late Ordovician *Himantia* Fauna on the upper Yangtze Platform, South China[J]. Science China: Earth Sciences, 2010, 40(9): 1154-1163.]

[128] Rohrssen M, Love G D, Fischer W, et al. Lipid biomarkers record fundamental changes in the microbial community structure of tropical seas during the Late Ordovician Hirnantian glaciation[J]. Geology, 2013, 41(2): 127-130.

[129] Melchin M J, Mitchell C E, Holmden C, et al. Environmental changes in the Late Ordovician - Early Silurian: review and new insights from black shales and nitrogen isotopes[J]. GSA Bulletin, 2013, 125(11/12): 1635-1670.

[130] Cooper R A, Sadler P M. The Ordovician period[M]//Gradstein F M, Ogg J G, Schmitz M, et al. The Geologic Time Scale. Amsterdam: Elsevier, 2012: 489-523.

[131] Finnegan S, Heim N A, Peters S E, et al. Climate change and the selective signature of the Late Ordovician mass extinction[J]. Proceedings of the National Academy of Sciences of the United States of America, 2012, 109(18): 6829-6834.

[132] Yan D T, Chen D Z, Wang Q C, et al. Large-scale climatic fluctuations in the latest Ordovician on the Yangtze block, South China[J]. Geology, 2010, 38(7): 599-602.

[133] Trotter J A, Williams I S, Barnes C R, et al. Did cooling oceans trigger Ordovician biodiversification? Evidence from conodont thermometry[J]. Science, 2008, 321(5888): 550-554.

[134] Moulton K, Berner R A. Quantification of the effect of plants on weathering: studies in Iceland[J]. Geology, 1998, 26(10): 895-898.

[135] Lenton T M, Crouch M, Johnson M, et al. First plants cooled the Ordovician[J]. Nature Geoscience, 2012, 5(2): 86-89.

[136] Jenkyns H C. Geochemistry of oceanic anoxic events[J]. Geochemistry, Geophysics, Geosystems, 2010, 11(3): Q03004.

[137] Percival L M E, Witt M L I, Mather T A, et al. Globally enhanced mercury deposition during the end-Pliensbachian extinction and Toarcian OAE: a link to the Karoo-Ferrar Large Igneous Province[J]. Earth and Planetary Science Letters, 2015, 428: 267-280.

[138] Percival L M E, Cohen A S, Davies M K, et al. Osmium isotope evidence for two pulses of increased continental weathering linked to Early Jurassic volcanism and climate change[J]. Geology, 2016, 44(9): 759-762.

[139] Dasgupta R. Ingassing, storage, and outgassing of terrestrial carbon through geologic time [J]. Reviews in Mineralogy and Geochemistry, 2013, 75(1): 183-229.

[140] Lee C T A, Shen B, Slotnick B S, et al. Continental arc - island arc fluctuations, growth of crustal carbonates, and long-term climate change[J]. Geosphere, 2013, 9(1): 21-36.

[141] Lee C T A, Lackey J S. Global continental arc flare-ups and their relation to long-term greenhouse conditions[J]. Elements, 2015, 11(2): 125-130.

[142] McKenzie N R, Horton B K, Loomis S E, et al. Continental arc volcanism as the principal driver of icehouse-greenhouse variability[J]. Science, 2016, 352(6284): 444-447.

[143] EvansD A D. Reconstructing pre-Pangean supercontinents[J]. GSA Bulletin, 2013, 125(11/12): 1735-1751.

[144] Li Z X, Bogdanova S V, Collins A S, et al. Assembly, configuration, and break-up history of Rodinia: a synthesis[J]. Precambrian Research, 2008, 160(1/2): 179-210.

[145] McKenzie N R, Hughes N C, Gill B C, et al. Plate tectonic influences on Neoproterozoic – early Paleozoic climate and animal evolution[J]. Geology, 2014, 42(2): 127-130.

[146] Buggisch W, Joachimski M M, Lehnert O, et al. Did intense volcanism trigger the first Late Ordovician icehouse? [J]. Geology, 2010, 38(4): 327-330.

[147] Qing H R, Veizer J. Oxygen and carbon isotopic composition of Ordovician brachiopods: implications for coeval seawater[J]. Geochimica et Cosmochimica Acta, 1994, 58(20): 4429-4442.

[148] Patzkowsky M E, Holland S M. Patterns of turnover in Middle and Upper Ordovician brachiopods of the eastern United States: a test of coordinated stasis[J]. Paleobiology, 1997, 23(4): 420-443.

[149] Herrmann A D, Patzkowsky M E, Pollard D. The impact of paleogeography, pCO_2, poleward ocean heat transport and sea level change on global cooling during the Late Ordovician[J]. Palaeogeography, Palaeoclimatology, Palaeoecology, 2004, 206(1/2): 59-74.

[150] Rosenau N A, Herrmann A D, Leslie S A. Conodont apatite $\delta^{18}O$ values from a platform margin setting, Oklahoma, USA: implications for initiation of Late Ordovician icehouse conditions[J]. Palaeogeography, Palaeoclimatology, Palaeoecology, 2012, 315-316: 172-180.

[151] Patzkowsky M E, Holland S M. Extinction, invasion, and sequence stratigraphy: patterns of faunal change in the Middle and Upper Ordovician of the eastern United States[M]//Witzke B J, Ludvigson G A, Day J. Paleozoic Sequence Stratigraphy: Views from the North American Craton, Volume 306. Boulder, Colorado: Geological Society of America, 1996: 131-142.

[152] Herrmann A D, MacLeod K G, Leslie S A. Did a volcanic megaeruption cause global cooling during the Late Ordovician? [J]. Palaios, 2010, 25(11/12): 831-836.

[153] Herrmann A D, Haupt B J, Patzkowsky M E, et al. Response of Late Ordovician paleoceanography to changes in sea level, continental drift, and atmospheric pCO_2 potential causes for long-term cooling and glaciation[J]. Palaeogeography, Palaeoclimatology, Palaeoecology, 2004, 210(2/3/4): 385-401.

[154] Frakes L A, Francis J E, Syktus J I. Climate Modes of the Phanerozoic: The History of the Earth's Climate over the Past 600 Million Years[M]. Cambridge: Cambridge University Press, 1992: 274.

[155] Brookfield M E. A mid-Ordovician temperate carbonate shelf-the Black River and Trenton Limestone Groups of southern Ontario, Canada[J]. Sedimentary Geology, 1988, 60(1/2/3/4): 137-153.

[156] Holland S M, Patzkowsky M E. Distal orogenic effects on peripheral bulge sedimentation; middle and upper Ordovician of the Nashville dome[J]. Journal of Sedimentary Research, 1997, 67(2): 250-263.

[157] Armstrong H A, Coe A L. Deep-sea sediments record the geophysiology of the Late Ordovician glaciation[J]. Journal of the Geological Society, 1997, 154(6): 929-934.

[158] Ramstein G. Climates of the earth and cryosphere evolution[J]. Surveys in Geophysics, 2011, 32(4/5): 329-350.

[159] Shaviv N J, Veizer J. Celestial driver of Phanerozoic climate? [J]. GSA Today, 2003, 13(7): 4-10.

[160] Luo G M, Algeo T J, Zhan R B, et al. Perturbation of the marine nitrogen cycle during the Late Ordovician glaciation and mass extinction[J]. Palaeogeography, Palaeoclimatology, Palaeoecology, 2016, 448: 339-348.

[161] Naqvi S W A, Yoshinari T, Jayakumar D A, et al. Budgetary and biogeochemical implications of N_2O isotope signatures in the Arabian Sea[J]. Nature, 1998, 394(6692): 462-464.

[162] Galloway J N. The global nitrogen cycle[M]//Holland H D, Turekian K K. Treatise on Geochemistry: Volume 8, Biogeochemistry. Oxford: Pergamon, 2003: 557-583.

[163] Mora C I, Driese S G, Colarusso L A. Middle to late Paleozoic atmospheric CO_2 levels from soil carbonate and organic matter[J]. Science, 1996, 271(5252): 1105-1107.

[164] Berner R A. A model for atmospheric CO_2 over Phanerozoic time[J]. American Journal of Science, 1991, 291(4): 339-376.

[165] Berner R A. GEOCARB II: a revised model of atmospheric CO_2 over Phanerozoic time[J]. American Journal of Science, 1994, 294(1): 56-91.

[166] Berner R A, Kothavala Z. GEOCARB III: a revised model of atmospheric CO_2 over Phanerozoic time[J]. American Journal of Science, 2001, 301(2): 182-204.

[167] 苏文博,何龙清,王永标,等. 华南奥陶—志留系五峰组及龙马溪组底部斑脱岩与高分辨综合地层[J]. 中国科学(D 辑), 2002,32(3):207-219. [Su Wenbo, He Longqing, Wang Yongbiao, et al. K-bentonite beds and high-resolution integrated stratigraphy of the uppermost Ordovician Wufeng and the lowest Silurian Longmaxi formations in South China[J]. Science in China (Series D), 2002, 32(3): 207-209.]

The Genesis of Hirnantian Glaciation and Paleo-Ocean Environment During Ordovician-Silurian Transition

YANG XiangRong, YAN DeTian, ZHANG LiWei, ZHANG Bao, XU HanWen, LIU WenHui, YUN JiaLin

Key Laboratory of Tectonics and Petroleum Resources Ministry of Education, China University of Geosciences, Wuhan 430070, **China**

Abstract: The Ordovician-Silurian transition was an interval which revealed major changes in the Earth´s biotic, climatic, and environmental systems, triggering the Hirnantian glaciation and end-Ordovician mass extinctions. The paleo-ocean environment experienced intense shift and exerted a crucial impact on the global cycles of carbon, molybdenum and sulfur during O-S transition. In addition, the weakness of continental weathering reduced ^{187}Os and ^{87}Sr flux, resulting in positive $\delta^{187}Os$ and $\delta^{87}Sr$ excursions. This first ice age, since the late Neoproterozoic, was the culmination of a cooling trend that had begun in the early or middle Ordovician, and was linked to some combination of reduced volcanic arc outgassing, enhanced silicate weathering, increased organic carbon burial and so on. There exist many problems about the genesis of Hirnantian glaciation, such as lacking in individual biostratigraphy which can control the carbonate platform in shallow water and mudstone in deep water simultaneously, as well as the high-precision analysis based on geochemical proxies and isochronous stratigraphic correlation. Meanwhile diagenesis, weathering and tectonic-thermal events also exerted an important impact on reconstruction of Hirnantian glaciation, resulting in inaccurate interpretation.

Key words: Hirnantian glaciation; paleo-ocean environment; end-Ordovician; mass extinctions